

Internal Protection of Transformer Windings Against Transient Surges Using ZnO Varistors

R. Shariatinasab, Z. Ejtemaei, J. Gholinezhad

Abstract - Power system overvoltages due to switching, lightning and other disturbances are the main problem for designers of the power transformers. Once some frequencies of the incoming surges match with some of the natural frequencies of transformer winding, the resonance phenomenon is expected in transformer winding. The resonant overvoltages may destroy the insulation between turns and cause to insulation failure or transformer damage. In this paper, the transformer winding is modeled based on the lattice diagram concept with variable parameters and the IEEE model of surge arresters has been utilized in order to perform the simulations. For internal protection of transformer windings, it is assumed that ZnO varistors are installed in parallel to the winding turns. Also the effect of ZnO varistors in reducing the voltage stress across the transformer winding has been investigated for the case of grounded and insulated neutral winding.

Index Terms - Zno oxide arrester, transient stresses, internal protection, transformer winding.

I. INTRODUCTION

POWER transformer is one of the essentially and also more expensive equipment of electrical networks which plays mainly role in the energy transmission and distribution. For this reason, transformers must be withstood facing with several electrical stresses. Among these stresses, lightning and switching voltages lead to form dangerous transient overvoltages which can destroy transformer insulation. Therefore, studying the transformers transient responses has been found significantly importance to obtain the highest reliability [1].

During last years, several studies have been carried out regarded to the modeling of transformer transients[1-3]. Unfortunately, most of these mentioned models are formed based on experimental results or complicated mathematical relations in order to identify model parameters that do not have enough accuracy [2, 3]. For example in calculating the

parameters of the winding ladder model [1-3], the designing characteristic is assumed constant during the winding, while these values are variable in different winding sections. In these approaches, the model parameters are calculated assuming that the winding height, winding width and the insulation thickness are fixed. So by changing the shape of the winding due to mechanical forces and electrical stresses, the calculating of transient parameters is impossible. Furthermore, in these methods must calculate five electrical elements in each turn of the winding as a result modeling of the real winding takes long time.

In this paper, ladder model with variable parameters and limited sections are used for modeling of the winding, which can use in insulation coordination studies and in identifying of the fault location by using the frequency response. Internal protection of transformer windings is performed using parallel zinc-oxide arrester. The case study is simulated in electromagnetic transient program EMTP/ATP and is analyzed the voltage distribution of the transformer winding for different states (the grounded winding and isolated winding). Also, the impact of surge arrester number and placement on reducing voltage stress is demonstrated.

II. THE VOLTAGE DISTRIBUTION ACROSS THE WINDING WITH VARIABLE PARAMETERS FOR EACH SECTION

For describing the transient model of heterogeneous windings [4], identifying of the fault location and partial discharge [5,6] by using the frequency response, the model of winding with variable parameters is provided. In [7] the method of calculating these parameters are described. The transformer characteristic and the model parameters are presented in Table I and Table II, respectively.

r , L , C and K are series resistance, inductance between turns, parallel capacity and series capacity of the windings, respectively. The winding ladder model with seven sections is shown in Fig. 1. In this paper, for observing the distribution of voltage under standard impulse and step wave, 10 kA amplitude, are used.

This work was supported by the University of Birjand.

H. Saboori, S. Dehghan, S. Jadid are with the Department of Electrical Engineering, University of Birjand, Birjand, Iran. (e-mail: Shariatinasab@birjand.ac.ir)

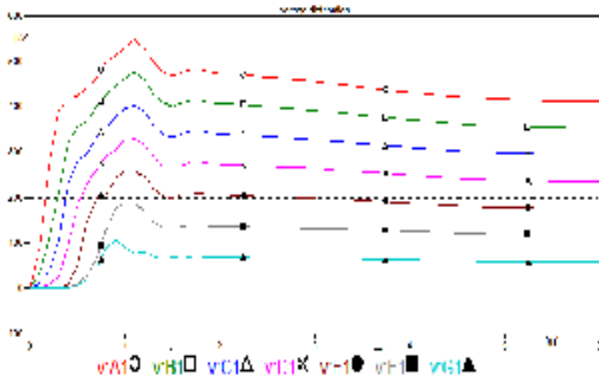


Fig. 5. The voltage distribution of the grounded winding with variable parameters under step wave

III. EMTP/ATP SIMULATION

A. Lightning Current

A Heidler function can be used to represent the lightning current waveform [8].

$$i(t) = \frac{I_p}{h} \frac{k^n}{1+k^n} e^{-\frac{t}{\tau_2}} \quad (1)$$

where I_p , n and η are the peak current, the current steepness factor and the peak current correction factor, respectively; and $k=t/\tau_1$; τ_1 and τ_2 are time constants that determine the rise time and decay time of the lightning waveform, respectively. Lightning current (10 kA, $8\mu s/20\mu s$) is shown in Fig. 6.

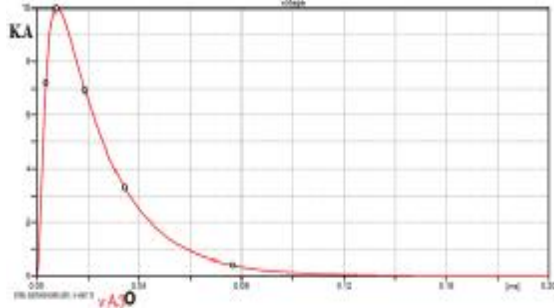


Fig. 6. Standard lightning waveshape (10 kA, $8\mu s/20\mu s$)

B. Transformer winding ladder model

In this paper, a ladder model consist of 7 sections (Fig. 1) is used that 2 sections of them are shown in Fig. 7. This model for insulation coordination studies and fault location recognizing and etc is used. Every part of the ladder grid represents a group of disks in disk winding and a few turns in the snails winding [9-11]. The proposed model is easier compared to the travelling wave-based models [12, 13] and the multi-wire transmission line theory [14-16], however it should be more accurately determined these parameters to predict the transient behavior of transformer winding.

The winding frequency response is depend on resistance, inductance and capacitance parameters of ladder grid. These parameters are defined as follows [17, 18]:

C_i : the earth capacitance that modeled the capacitance

between the winding and tank (nF).

K_i : the series capacitance that modeled the capacitance between the i th and $(i-1)$ th sections (nF).

L_i : self inductance of the i th section (mH).

r_i : the series resistance of the i th section (k Ω).

The winding frequency response is related to the winding physical structure and characteristic, thus the change of physical structure of the winding caused changing these parameters, the frequency response and time response in transient. Therefore, the accurate calculation of these parameters play an important role in determining the exact model.

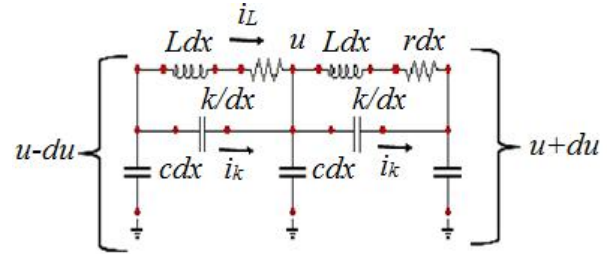


Fig. 7. The lattice diagram model of transformer winding

C. Arrester modeling

Surge arrester helps to reduce lightning overvoltages. This device is modelled based on its nonlinear voltage–current characteristic. Surge arresters are one of the most commonly used equipment in protection and insulation coordination of various types of electrical systems and devices. The IEEE has recommended a standard frequency dependent surge arrester model [19], as shown in Fig. 8.

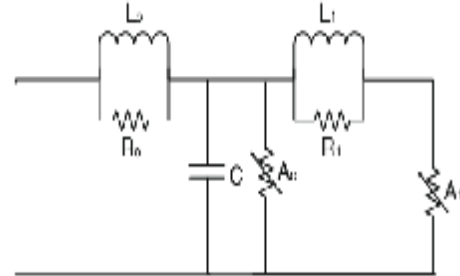


Fig. 8. IEEE model of surge arrester

Metal oxide varistor (MOV) are most popular used arresters. The arrester must spark over at a given level and carry the impulse current to ground. The arrester is able to reset when the applied voltage returns to normal. Linear parameters of Fig. 8 are determined as follows [20]:

$$\begin{aligned} L_0 &= 0.2 \frac{d}{n} (\text{mH}), R_0 = 100 \frac{d}{n} (\text{W}) \\ L_1 &= 15 \frac{d}{n} (\text{mH}), R_1 = 65 \frac{d}{n} (\text{W}) \\ C_0 &= 100 \frac{n}{d} (\text{pF}) \end{aligned} \quad (2)$$

Where, d is height of the arrester (m) and n is the number of parallel columns of MO disks. Great features that MOV were chosen are low residual voltage, short response time to

transients, high thermal stability and high energy absorption capacity when tested by transient and temporary overvoltages. According to use a transformer (1600 kVA, 20/0.4 kV) along to disk windings (38 disks), and 20 turns per disc (a total of 760 turns), the voltage level of 20 kV is used for the nominal voltage of arrester. The arrester residual voltage is shown in Fig. 9 under standard lightning impulse (Fig. 6).

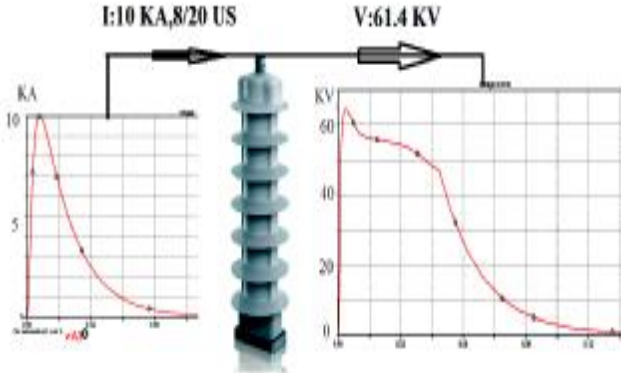


Fig. 9. The arrester residual voltage under standard lightning impulse

IV. PROTECTION OF TRANSFORMER WINDINGS USING ZNO VARISTORS

In previous section, the voltage distribution of transformer winding described and it was found that depending on the conditions, the winding is exposed to various types of stress. Overvoltage protection of transformer windings has an important role in designing of transformer.

EMTP simulation performed to protect the transformer windings under lightning and switching overvoltages. The effect of surge arresters in protecting of the transformer windings is analyzed under three protection arrangement of arrester connection to the windings as shown in Fig. 10. It is noted that the winding model with variable parameters has been used.

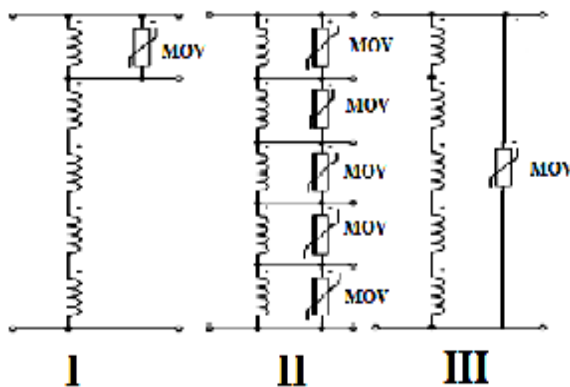


Fig. 10. Different configurations of installing ZnO varistors for protection of transformer winding

A. The first protective arrangement of arrester connection to the winding (I)

In this protective arrangement, only one part of the winding is parallel to the arrester. Depending on the conditions and the type of voltage distribution of the winding, the arrester is used

to protect the winding. For example, in the grounded winding because of appearing the greatest stress in the first part, the arrester is used in this section and in the isolated winding, the arrester is used in the manus according to evidence the greatest transient stress in this part. Figs. 11 and 12 shown the voltage distribution of the grounded winding under standard lightning impulse (10 kA, 8 μ s /20 μ s). The peak magnitude of overvoltage is reduced in parts of winding that is parallel with surge arrester while the overvoltage is increased on the other parts of winding due to changing the voltage distribution of winding because of presence of arrester which may cause damaging of the dielectric.

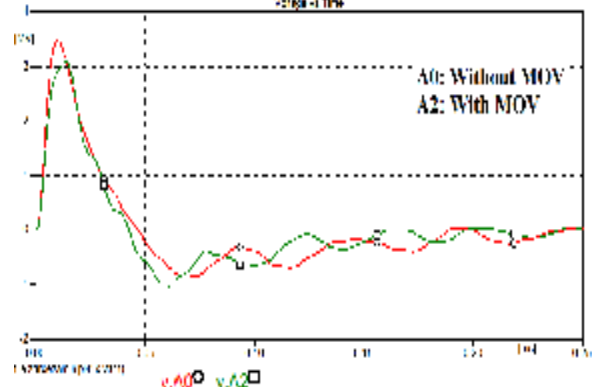


Fig. 11. The voltage distribution across the grounded winding equipped with protection configuration I installed across the first turns of winding.

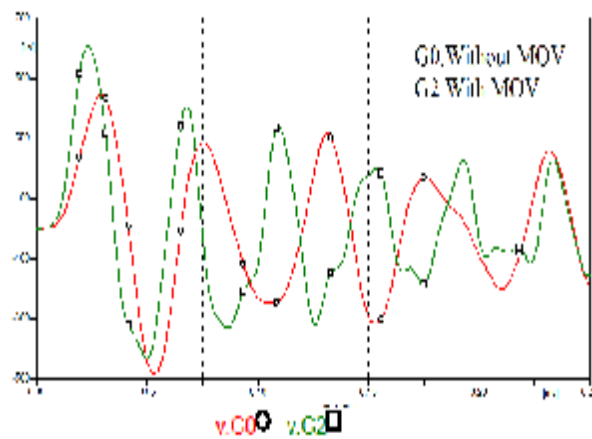


Fig. 12. The voltage distribution across the isolated winding equipped with protection configuration I installed across the end turns of winding.

Figs. 13 and 14 shown the voltage distribution of the isolated winding in the first and end parts of winding, respectively. It is clear from Fig. 13 that the peak magnitude of overvoltage is not changing in first parts of winding and both waveforms are nearly coincident, although surge arrester is parallel with winding at the end parts.

According to Fig. 14, the effect of this protection arrangement on oscillations damping and reducing the peak magnitude of overvoltage is negligible. The values of peak transient overvoltage in various sections of winding are provided in Table III. The effect of surge arrester on overvoltages is shown with negative and positive values ΔV .

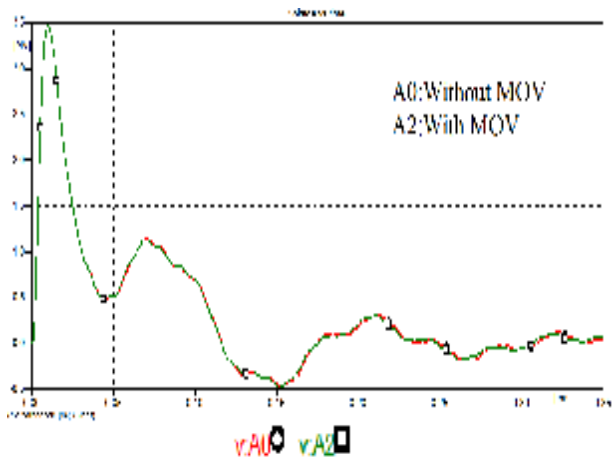


Fig. 13. The voltage distribution across the isolated winding equipped with protection configuration I installed across the first turns of the winding.

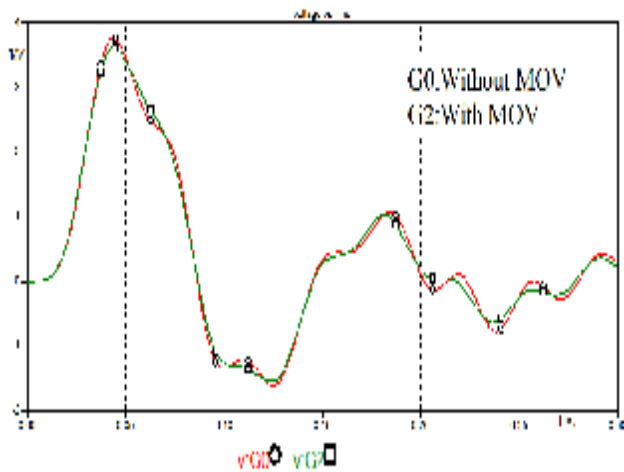


Fig. 14. The voltage distribution across the isolated winding equipped with protection configuration I across the end turns of winding

G, overvoltage decreased 0.15 MV in both sections G and H. Generally voltage of the grounded winding more increased than the isolated winding in without MOV sections.

B. The second protective configuration of arrester connection to the winding (II)

In this protective arrangement, various parts of the winding are parallel to the arrester. Figs. 15 and 16 shown the voltage distribution of the isolated winding and grounded winding, respectively. In this method, overvoltage has been reduced about several hundred kV and the oscillations have been damped. The voltage distribution of the winding is non-uniform and it's depend on the natural frequencies of the winding and entrance kind of transient stress. This method is useful against transients caused by local resonant, system disturbances, switching and lightning.

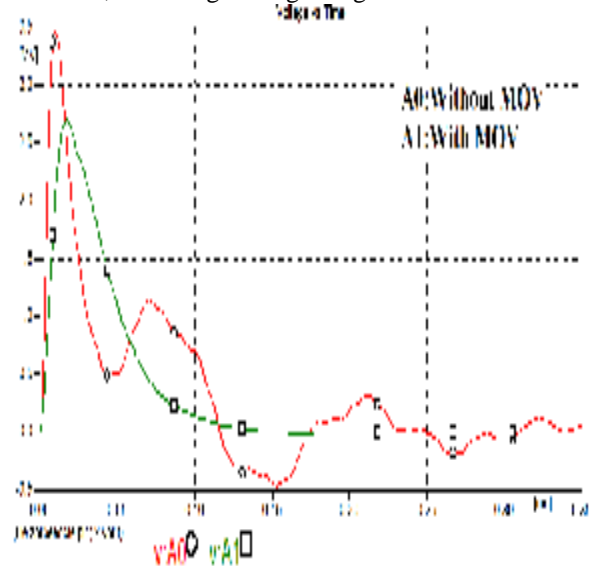


Fig. 15. The voltage distribution across the isolated winding equipped with protection configuration II across the first turns of winding

TABLE III

THE PROTECTION OF TRANSFORMER WINDING IN THE CASE OF THE FIRST PROTECTION CONFIGURATION

| Section | The grounded winding | | | The isolated winding | | |
|---------|----------------------|---------------|-----------------|----------------------|---------------|-----------------|
| | Without MOV (MV) | With MOV (MV) | ΔV (MV) | Without MOV (MV) | With MOV (MV) | ΔV (MV) |
| A | 3.4667 | 3.0963 | 0.3704 | 3.4618 | 3.4618 | 0 |
| B | 2.3439 | 3.0468 | -0.7029 | 2.8456 | 2.8831 | -0.0375 |
| C | 2.4892 | 3.6841 | -1.1948 | 2.9429 | 2.9948 | -0.0519 |
| D | 1.6389 | 2.09111 | -0.4522 | 3.1579 | 3.1592 | -0.0013 |
| E | 1.1127 | 1.5300 | -0.4173 | 3.4137 | 3.4385 | -0.0248 |
| F | 0.9568 | 1.3040 | -0.3471 | 3.5457 | 3.5738 | -0.0281 |
| G | 0.4423 | 0.60548 | -0.1631 | 3.7751 | 3.6234 | 0.1517 |
| H | 0 | 0 | 0 | 3.8143 | 3.6650 | 0.1493 |

It is observed that in first protection arrangement only the peak values of overvoltage is decreased in parts of winding that is parallel with surge arrester while the overvoltage is increased on the other parts of winding. In grounded winding with presence of arrester in section A, overvoltage reduced 0.37 MV and the biggest overvoltage occurred in section C. Also in isolated winding with attendance of arrester in section

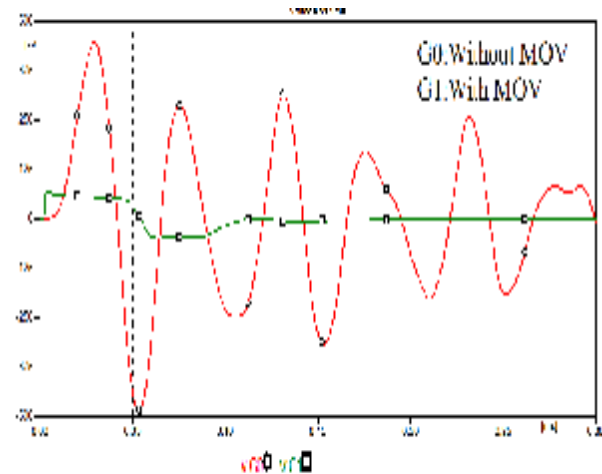


Fig. 16. The voltage distribution across the grounded winding equipped with protection configuration II across the end turns of winding.

It is clear that the reducing peak values of overvoltage and oscillations damping in the grounded winding is more occurred

than isolated winding and it is about several MV. The values of peak transient overvoltage in various sections of winding are provided in Table IV. As regards H section is grounded its voltage is equal to zero. Despite the effective protection, this method will be more expensive than other methods. According to ΔV , it is clear that reducing voltage in various sections occurred. In isolated winding the greatest reduction of voltage occurred in sections G and H about 1.04 and 1.07 MV, respectively. Also, in grounded winding the greatest reduction of voltage occurred in sections A and C about 2.98 and 2.14 MV, respectively.

TABLE IV
THE PROTECTION OF TRANSFORMER WINDING IN THE CASE OF SECOND PROTECTION CONFIGURATION

| Section s | The grounded winding | | | The isolated winding | | |
|-----------|----------------------|---------------|-----------------|----------------------|---------------|-----------------|
| | Without MOV (MV) | With MOV (MV) | ΔV (MV) | Without MOV (MV) | With MOV (MV) | ΔV (MV) |
| A | 3.4667 | 0.4785 | 2.9881 | 3.4618 | 2.7046 | 0.7572 |
| B | 2.3439 | 0.4120 | 1.9319 | 2.8456 | 2.6551 | 0.1905 |
| C | 2.4892 | 0.3448 | 2.1445 | 2.9429 | 2.6628 | 0.2801 |
| D | 1.6389 | 0.2766 | 1.3623 | 3.1579 | 2.6173 | 0.5406 |
| E | 1.1127 | 0.2078 | 0.9048 | 3.4137 | 2.6277 | 0.7860 |
| F | 0.9568 | 0.1392 | 0.8176 | 3.5457 | 2.6760 | 0.8697 |
| G | 0.4423 | 0.0691 | 0.3731 | 3.7751 | 2.7238 | 1.0472 |
| H | 0 | 0 | 0 | 3.8143 | 2.7376 | 1.0767 |

C. The third protective arrangement of arrester connection to the winding (III)

In this protective arrangement, all of parts of the winding are parallel to the one arrester and it is most commonly used protective method. In this method not required to exit additional taps during the transformer windings for connection to arrester and only the input and output windings are used to connect arrester. Figs. 17 and 18 demonstrated the voltage distribution of the isolated winding and grounded winding, respectively.

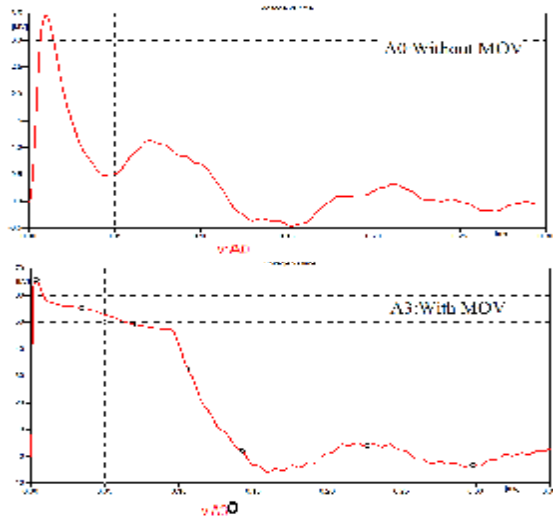


Fig. 17. The voltage distribution across the isolated winding equipped with protection configuration III across the first turns of winding.

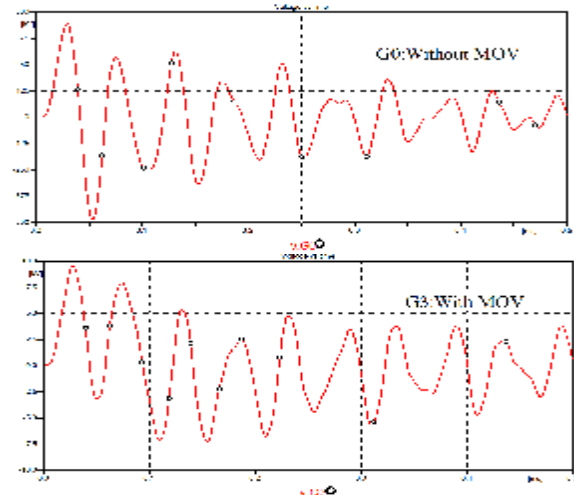


Fig. 18. The voltage distribution across the grounded winding equipped with protection configuration III across the end turns of winding.

It is observed that the decreasing peak values of overvoltage and oscillations damping are more than the previous methods and the peak magnitude of overvoltage is decreased about several MV specially in the end parts of the isolated winding. So in this way the oscillating voltage gradient decreased as a result insulation risk reduced. The values of peak transient overvoltage in various sections of winding is provided in Table V.

TABLE V
THE PROTECTION OF TRANSFORMER WINDING IN THE CASE OF THE THIRD PROTECTION CONFIGURATION

| Section s | The grounded winding | | | The isolated winding | | |
|-----------|----------------------|---------------|-----------------|----------------------|---------------|-----------------|
| | Without MOV (MV) | With MOV (MV) | ΔV (MV) | Without MOV (MV) | With MOV (MV) | ΔV (MV) |
| A | 3.4667 | 0.0657 | 3.4010 | 3.4618 | 0.0657 | 3.3961 |
| B | 2.3439 | 0.0597 | 2.2841 | 2.8456 | 0.0994 | 2.7462 |
| C | 2.4892 | 0.0581 | 2.4312 | 2.9429 | 0.1003 | 2.8425 |
| D | 1.6389 | 0.0383 | 1.6006 | 3.1579 | 0.1083 | 3.0496 |
| E | 1.1127 | 0.0238 | 1.0888 | 3.4137 | 0.1132 | 3.3005 |
| F | 0.9568 | 0.0203 | 0.9365 | 3.5457 | 0.1152 | 3.4305 |
| G | 0.4423 | 0.0096 | 0.4327 | 3.7751 | 0.1173 | 3.6537 |
| H | 0 | 0 | 0 | 3.8143 | 0.1185 | 3.6957 |

It is clear that the most decreasing peak values of overvoltage occurred in the third protection arrangement compared with other arrangements, so that the voltage been decreased more than 3 MV for the most parts. In grounded winding the greatest reduction of voltage occurred in sections A, B and C about 3.4, 2.28 and 2.43 MV, respectively.

V. THE EFFECT OF ARRESTER TYPE ON PROTECTION OF TRANSFORMER WINDING

Three different type of arrester are used for comparing the effect of kind of arrester on reducing and voltage oscillations damping. The various parameters of IEEE surge arrester model are obtained from manufacturer catalog. According to

previous section, the protection arrangement III has a most protective role in winding with the lowest number of arrester. As a result this arrangement is used for arrester sensitivity analysis. EMTP simulation performed as shown in Fig. 19 which in any case only one of the arresters is parallel to winding.

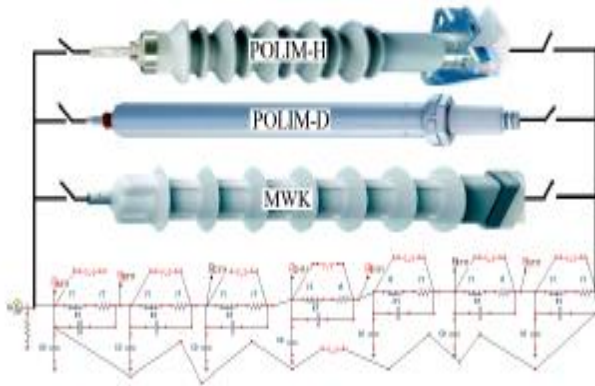


Fig. 19. The winding protection with different ABB arresters.

The different parameters of arrester are calculated with regard to (2) in 20 kV voltage level. These parameters are shown in Table VI.

TABLE VI
PARAMETERS OF THE IEEE MODEL FOR DIFFERENT ARRESTERS

| Arrester type | MWK | POLIM-D | POLIM-H |
|--------------------|--------------|--------------|--------------|
| L_0 (mH) | 0.0000614 | 0.000107 | 0.000072 |
| L_1 (mH) | 0.004605 | 0.008025 | 0.0054 |
| R_0 (Ω) | 30.7 | 53.5 | 36 |
| R_1 (Ω) | 19.995 | 34.775 | 23.4 |
| C(F) | 0.0003257329 | 0.0001869159 | 0.0002777778 |

Figs. 20 and 21 shown different protection levels of arresters, at first and the end of winding sections.

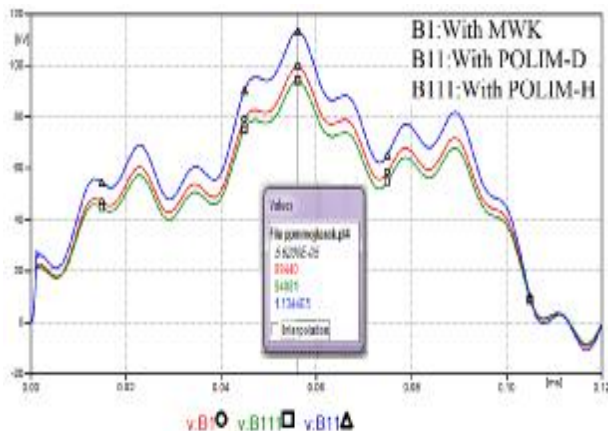


Fig. 20. The protection level of different arresters at the first turns of the isolated winding

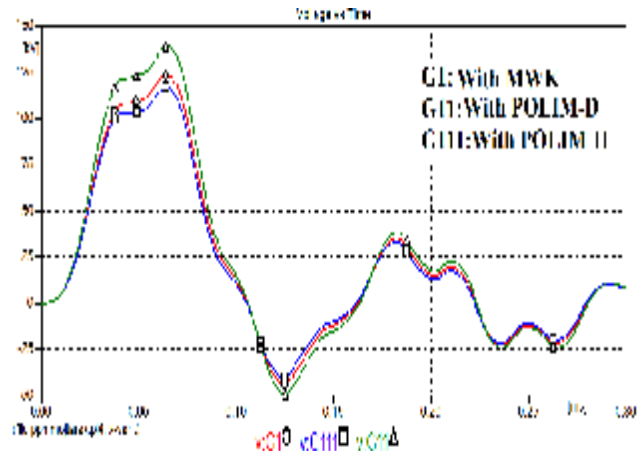


Fig. 21. The protection level of different arresters at the end turns of the isolated winding.

It is observed that overvoltage with POLIM-H arrester is more reduced than other arrester models. The voltage distribution of different sections shown in Table VII. It is clear that all arresters had great protective performance. According to case study characteristic (the insulation class, economic considerations, thermal, mechanical and physical properties) can be used from different surge arresters to protect transformer windings against voltage stresses.

TABLE VII
THE PROTECTION LEVELS OF DIFFERENT ARRESTERS IN ISOLATED WINDING

| Section | Voltage (MV) | | | |
|---------|--------------|----------|--------------|--------------|
| | Without MOV | With MWK | With POLIM-D | With POLIM-H |
| A | 3.4618 | 0.0657 | 0.0769 | 0.0630 |
| B | 2.8456 | 0.0994 | 0.1134 | 0.0940 |
| C | 2.9429 | 0.1003 | 0.1153 | 0.0953 |
| D | 3.1579 | 0.1083 | 0.1229 | 0.1022 |
| E | 3.4137 | 0.1132 | 0.1283 | 0.1067 |
| F | 3.5457 | 0.1152 | 0.1307 | 0.1086 |
| G | 3.7751 | 0.1173 | 0.1332 | 0.1107 |
| H | 3.8143 | 0.1185 | 0.1347 | 0.1118 |

It is observed that the voltage is more decreased at the end section of isolated winding with all three arrester. The most overvoltage occurred in section H that is about 3.8143 MV and it became about 0.1185, 0.1347 and 0.1118 MV in presence of MWK, POLIM-D and POLIM-H arresters, respectively.

Figs. 22 and 23 demonstrated different protection levels of arresters in the grounded winding. Also, here the overvoltage with POLIM-H arrester is more reduced than the other arrester models.

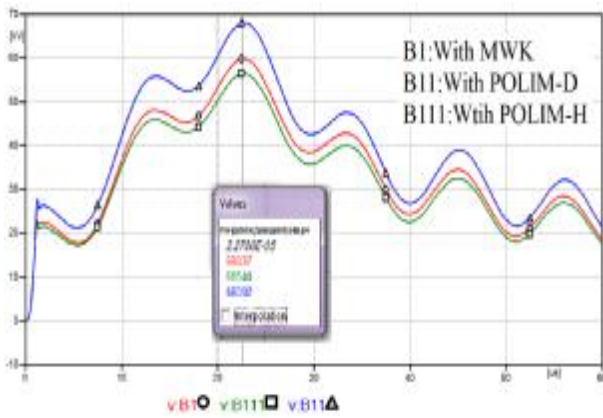


Fig. 22. The protection levels of different arresters at the first turns of the grounded winding.

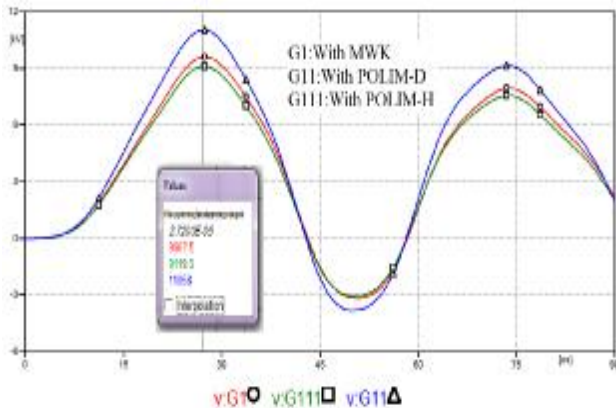


Fig. 23. The protection levels of different arresters at the end turns of the grounded winding.

The peak values of overvoltage in various sections come in Table VIII.

TABLE VIII
THE PROTECTION LEVELS OF DIFFERENT ARRESTERS IN THE GROUNDED WINDING

| Section | Voltage (MV) | | | |
|---------|--------------|----------|--------------|--------------|
| | Without MOV | With MWK | With POLIM-D | With POLIM-H |
| A | 3.4667 | 0.0657 | 0.0769 | 0.0631 |
| B | 2.3439 | 0.0597 | 0.0680 | 0.0565 |
| C | 2.4892 | 0.0581 | 0.0671 | 0.0553 |
| D | 1.6389 | 0.0383 | 0.0435 | 0.0361 |
| E | 1.1127 | 0.0238 | 0.0274 | 0.0227 |
| F | 0.9568 | 0.0203 | 0.0235 | 0.0194 |
| G | 0.4423 | 0.0096 | 0.0110 | 0.0091 |
| H | 0 | 0 | 0 | 0 |

VI. CONCLUSIONS

From the results, it was found that the initial and final voltage distribution is independent of the type of winding (the grounded star or delta) and it has the maximum amount in the first section of winding. While the maximum voltage stress in voltage oscillations occurred in the end and first sections in the isolated and grounded windings, respectively.

In first protective arrangement, the peak magnitude of overvoltage is reduced in part of winding that is parallel to surge arrester while the overvoltage is increased on the other parts of winding so that the overvoltages are about 1.19 and 0.051 MV in the grounded and isolated windings, respectively, that is not appropriate. In second protective arrangement, overvoltages have been reduced and the oscillations have been damped in different sections. So that the peak values of overvoltage are reduced about 3 MV and 1 MV for the grounded and isolated windings, respectively. But the number of useful arresters is high and it is essential differnt taps during the transformer windings as a result the costs will increase. In third protective arrangement, transformer winding protected with the lowest number of arrester. The overvoltage reducing and voltage oscillations damping are more than the previous protective arrangements so that the peak values of overvoltage are reduced more than 3 MV in the most parts of the isolated winding, while ti is noted that this arrangement is not effective against the local resonant.

In the following a sensitivity analysis is performed. Owing the results, the overvoltage with POLIM-H arrester is more reduced than the other arrester models, ae a result use a one arrester (POLIM-H model) parallel to the transformer winding is the best protection method in studied transformer winding.

VII. REFERENCES

- [1] M. Bigdeli, D. Azizian, H. Bakhshi, and E. Rahimpour, "Identification of transient model parameters of transformer using genetic algorithm," In Power System Technology (POWERCON), 2010 International Conference on, pp. 1-6, October 2010.
- [2] I. Wolff, *Maxwellsche Theorie: Grundlagen und Anwendungen*. Berlin: Springer-Verlag, 1997.
- [3] A. Gray, *Absolute Measurements in Electricity and Magnetism*. New York: Dover, 1967.
- [4] V. Rashtchi, E. Rahimpour, and E. Rezapour, "Using a genetic algorithm for parameter identification of transformer R-L-C-M model," *Elect. Eng.*, vol. 88, no. 5, pp. 417-422, 2006.
- [5] Coffeen, Larry, Jeffrey Britton, and Johannes Rickmann. "A new technique to detect winding displacements in power transformers using frequency response analysis." *Power Tech Conference Proceedings, IEEE Bologna*. Vol. 2. , 2003.
- [6] Rahimpour, Ebrahim, Mehdi Jabbari, and Stefan Tenbohlen. "Mathematical comparison methods to assess transfer functions of transformers to detect different types of mechanical faults." *Power Delivery, IEEE Transactions* vol.4, no.24, pp. 2544-2555,2005.
- [7] Shabestary, M.M. ; Ghanizadeh, A.J. ; Gharehpetian, G.B. ; Agha-Mirsalim, M. " Ladder Network Parameters Determination Considering Nondominant Resonances of the Transformer Winding," *IEEE Transactions on Power Delivery*,vol.29, no.1, pp. 108 - 117, 21 January 2014.
- [8] Heidler, F., J. M. Cvetic, and B. V. Stanic. "Calculation of lightning current parameters," *Power Delivery, IEEE Transactions on* vol.14, no. 2, pp.399-404, 1999
- [9] N. Abeywickrama, Y. V. Serdyuk, and S. M. Gubanski, "Exploring possibilities for characterization of power transformer insulation by frequency response analysis (FRA)," *IEEE Trans. Power Del.* , vol. 21,no. 3, pp. 1375-1382, Jul. 2006.
- [10] N. Abeywickrama, "Effect of Dielectric and Magnetic Material Characteristics on Frequency Response of Power Transformers," Ph.D. dissertation, Dept. Mater. Manuf. Technol., Chalmers Univ. of Technol.,Gothenburg, Sweden, 2007.

- [11] M. Florkowski and J. Furgal, "Detection of transformer winding deformations based on the transfer function measurements and simulations," *Meas. Sci. Technol.*, vol. 14, no. 11, pp. 1986–1992, 2003.
- [12] A. Shintemirov, W. H. Tang, Z. Lu, and Q. H. Wu, "Simplified transformer winding modeling and parameter identification using particle swarm optimizer with passive congregation," *App. Evol. Comput.*, vol. 4448, pp. 145–152, 2007.
- [13] A. Shintemirov, W. H. Tang, and Q. H. Wu, "A hybrid winding model of disc-type power transformers for frequency response analysis," *IEEE Trans. Power Del.*, vol. 24, no. 2, pp. 730–739, Apr. 2009.
- [14] S. M. H. Hosseini, M. Vakilian, and G. B. Gharehpetian, "Comparison of transformer detailed models for fast and very fast transient studies," *IEEE Trans. Power Del.*, vol. 23, no. 2, pp. 733–741, Apr. 2008.
- [15] H. Sun, G. Liang, X. Zhang, and X. Cui, "Modeling of transformer windings under very fast transient overvoltages," *IEEE Trans. Electromagn. Compat.*, vol. 48, no. 4, pp. 621–627, Nov. 2006.
- [16] M. Popov, L. van der Sluis, R. P. P. Smeets, and J. L. Roldan, "Analysis of very fast transients in layer-type transformer windings," *IEEE Trans. Power Del.*, vol. 22, no. 1, pp. 238–247, Jan. 2007.
- [17] P. Karimifard, G. B. Gharehpetian, and S. Tenbohlen, "Localization of winding radial deformation and determination of deformation extent using vector fitting-based estimated transfer function," *Eur. Trans. Elect. Power*, vol. 19, no. 5, pp. 749–762, Jul. 2009.
- [18] P. Karimifard, G. B. Gharehpetian, A. J. Ghanizadeh, and S. Tenbohlen, "Estimation of simulated transfer function to discriminate axial displacement and radial deformation of transformer winding," *COMPEL: Int. J. Comput. Math. Elect. Electron. Eng.*, vol. 31, no. 4, pp. 1277–1292, 2012.
- [19] IEEE Guide for the Application of Metal-Oxide Surge Arresters for Alternating-Current Systems. IEEE Std C62.22-1997, 1998.
- [20] J. A. Martinez and D. W. Durbak, "Parameter determination for modeling systems transients—Part V: Surge arresters," *IEEE Trans. Power Del.*, vol. 20, no. 3, pp. 2073–2078, Jul. 2005.

